

Evidence for Nucleon Clustering from High-Energy Reactions

M. LEFORT, J. P. COHEN, H. DUBOST, AND X. TARRAGO

*Laboratoire de Chimie Nucléaire, Faculté des Sciences de Paris-Orsay, France**

(Received 5 May 1965)

The telescope method was used with solid-state detectors for measuring angular and energy distributions of complex particles emitted in nuclear reactions induced by 157-MeV protons on heavy nuclei (Ag, Au, Bi, Th). Both an isotropic and a forward-peaked emission of ^4He , tritons, and deuterons were observed. Yields of ^4He were found to be very low at the back angles. The components of the above particle spectra emitted at forward angles are interpreted in terms of a direct-interaction mechanism on " α clusters" in the surface, and a Monte Carlo calculation was performed to compute the yield of " α clusters" knocked out by prompt cascade nucleons. The tritons and ^3He particles might partly be ejected by a double pickup process, partly by a stripping mechanism on " α clusters."

I. INTRODUCTION AND EXPERIMENTAL EQUIPMENT

IN recent years we have studied by different methods the emission of α particles from targets bombarded by high-energy protons. Very recently we have extended our experiments to energy and angular distributions for emission of deuterons, tritons, and ^3He from silver and gold targets. All our data show that in all cases, two processes occur, except perhaps for ^3He particles. The first one, isotropically distributed in the center-of-mass system, has been attributed to an evaporation mechanism from highly excited nuclei. The second one, peaked in the forward direction, is related to a more direct interaction, whose characteristics depend on the nature of the particle. We believe that ^4He particles are ejected by a "knockout" collision and that this is some evidence for nucleons clustering into α substructures. On the other hand, deuterons and tritons are mainly emitted through secondary pickup mechanisms, and the forward emission for ^3He might be explained either by a double pickup process or by stripping on ^4He .

The experimental equipment has already been described in principle,¹ but we have made some improvements on the electronics. A ΔE - E counter telescope was still used but we also used two ΔE counters for coincidence signals. A block diagram of the electronics is shown in Fig. 1. Pulses from both ΔE detectors are put in a fast coincidence circuit after double differentiation. Fast coincidence signals are sent to a slow coincidence circuit which delivers a pulse when a signal is coming from the sum circuit ($\Delta E_1 + \Delta E_2 + E$) after a discriminator. Pulses from the slow coincidence circuits open gates on linear-analysis channels both for sum ($\Delta E_1 + \Delta E_2 + E$) and for ($\Delta E_1 + \Delta E_2$) signals. A 1024-channel analyzer is used for two-dimensional analysis over 16 $\Delta E/\Delta X$ intervals. Total-energy pulses are distributed through 64 channels in each interval.

The energy calibration of the counters was done by

selecting a narrow width for ΔE . The corresponding energy was therefore well defined by the relation between dE/dX and E . We checked the linear response of the E detectors through all the energy range from 2 to 80 MeV for deuterons, tritons, and helium ions.

II. EXPERIMENTAL RESULTS AND DISCUSSION ON THE ANGULAR DISTRIBUTIONS AND THE CROSS SECTIONS FOR THE ISOTROPIC PROCESS

Differential cross sections have been measured at the angles $\theta = 20^\circ, 45^\circ, 60^\circ, 90^\circ, 105^\circ, 135^\circ$, and 160° for helium ions, tritons, and deuterons. However, it should be mentioned that the detector's thickness was not sufficient to measure the energy spectra up to the highest energy. The limits are around 70 to 80 MeV for helium ions, 50 to 60 MeV for tritons, and 40 MeV for deuterons.

It can be seen, in Figs. 2 and 3, that the cross-section value does not exhibit any variation between 160° and 135° , and we have assumed that all particles emitted at these two angles belong to an isotropic process. In order to calculate the center-of-mass correction, the mean excitation energy was estimated to be 90 MeV and a corresponding momentum was attributed to the recoiling nucleus. It was therefore possible to calculate integrated total cross sections for the isotropic process, which are given in Table I. These values for tritium are in good agreement with a set of data obtained by a very different technique, which consisted of measuring the tritium content in stacked foils following bombardments by 155-MeV protons.²

TABLE I. Cross section in millibarns for the particles emitted through an "isotropic" process from targets bombarded at 157 MeV.

	Thorium	Bismuth	Gold	Silver
^4He	37 ± 7	45 ± 7	72 ± 8	> 120
^3He		< 2.5	2.5	8.5
^3H	20 ± 3		18 ± 3	18 ± 3
^2H			32 ± 5	69 ± 8

* Postal address: Laboratoire Joliot-Curie, B.P. n° 1, Orsay (S. & O.) France.

¹ H. Dubost, M. Lefort, J. Peter, and X. Tarrago, Phys. Rev. **136**, B1618 (1964).

² H. Dubost, thesis, Paris-Orsay, 1965 (unpublished).

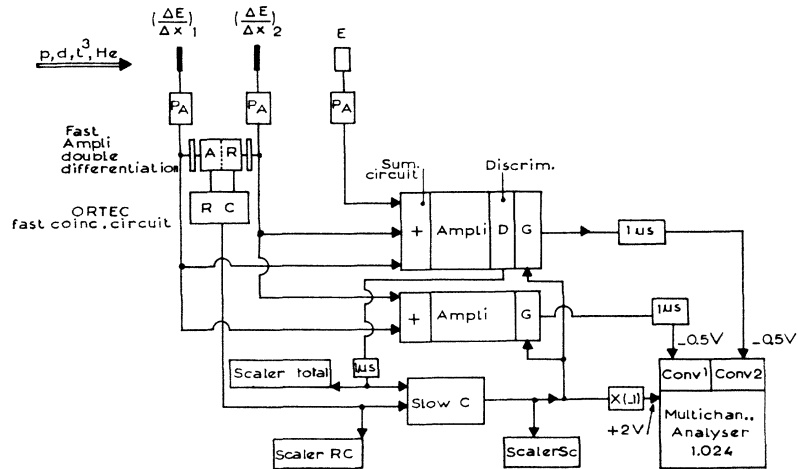


FIG. 1. Electronics block diagram.

Electronics Block Diagram

On the other hand, energy distributions of the particles emitted in the backward direction (160° or 135°) look very similar to evaporation spectra. The main features obtained for gold targets are shown in Fig. 4. It is interesting that the threshold values are far below the Coulomb barrier (12.8 MeV for ^4He and 6 MeV for tritons and deuterons, as compared with 23 to 26 MeV and 12–15 MeV, respectively, for the calculated Coulomb barriers).

However, this result, as well as similar data from Muto *et al.*,³ can be explained in a rather satisfactory manner if one applies the statistical evaporation theory with correct values for the cross section of the inverse process. Calculations have been carried out by Da

Silveira⁴ for α particles and by Dubost² for tritons, starting with a distribution of excited nuclei given by the cascade calculations. Usual values were used for the parameters r_0 (1.3 F) and a ($A/15$ for Bi) but the dependence of σ_{inverse} on the energy was treated by an analytical function which follows very closely the continuum theory, especially for the low-energy values. Calculations of the evaporation probability for ^3He from gold or bismuth yield a very low cross section of less than 1 mb, although for silver the Coulomb-barrier inhibition is not so strong. The experimental data in Table I are in good agreement with these predictions.

III. FRACTIONS EMITTED IN THE FORWARD DIRECTION. ENERGY DISTRIBUTIONS

After subtracting the evaporation contribution at all angles, a sizable particle emission still exists at

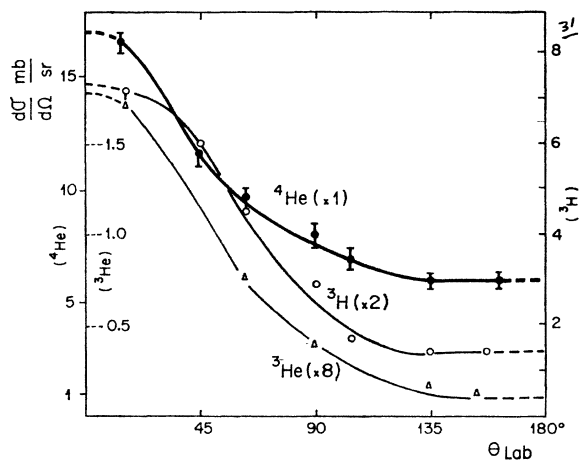


FIG. 2. Angular distribution in the laboratory of ^4He , ^3He , and ^3H emitted from gold targets. Bombarding energy 157-MeV protons. Notice different scales for ^4He , ^3He ($\times 8$) and ^3H ($\times 2$).

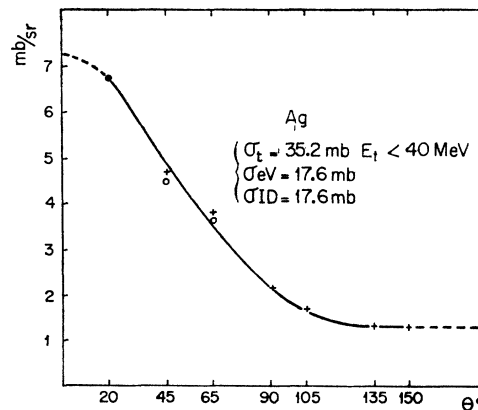


FIG. 3. Angular distribution for tritons from silver.

³ J. Muto, H. Itoh, K. Okamo, N. Shiomi, K. Fukuda, Y. Omori, and M. Kihara, Nucl. Phys. 47, 19 (1963).

⁴ R. Da Silveira, thesis, Paris-Orsay, 1965 (unpublished); M. Lefort and R. Da Silveira, Nucl. Phys. (to be published).

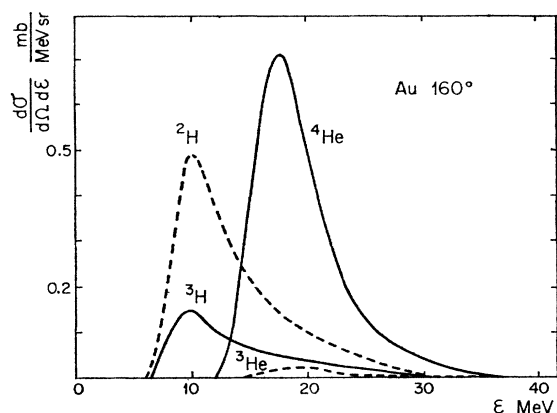


FIG. 4. Energy distributions in the backward angles of ${}^4\text{He}$, ${}^3\text{He}$, and ${}^3\text{H}$ from gold.

forward angles for helium ions, tritons, and deuterons, and its magnitude is calculated by integrating over the angles in the equation

$$\frac{d\sigma}{dE} = 2\pi \int_{\theta=0^\circ}^{\theta=105^\circ} \frac{d^2\sigma}{dE d\Omega} \sin\theta d\theta,$$

since the nonisotropic process gives a contribution only between 0 and 105° . One can see by comparing Table II and Table I that the order of magnitude of the

TABLE II. Cross sections in millibarns for the particles emitted through a "nonisotropic" process from targets bombarded at 157 MeV.

	Th	Bi	Au	Ag
${}^4\text{He}$ ($E < 80$ MeV)	44	37 ± 5	37	...
${}^3\text{He}$ ($E < 70$ MeV)		4.5	4.1	3.5
${}^3\text{H}$ ($E < 50$ MeV)	24		23.5	17.5

nonisotropic process is as large as that for the isotropic evaporation for ${}^4\text{He}$ and tritons, and is larger for

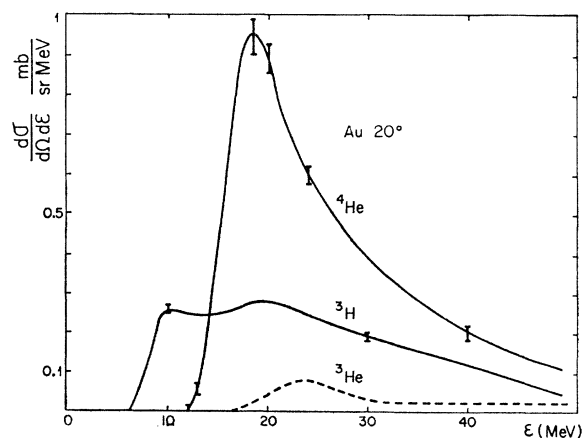


FIG. 5. Energy distribution at $\theta_{\text{lab}} = 20^\circ$ of ${}^4\text{He}$, ${}^3\text{He}$, and ${}^3\text{H}$ from gold.

${}^3\text{He}$. No value can be given for deuterons because the energy distribution cannot be measured higher than 30 MeV.

The energy spectra extend over a wide range in energy and our detector arrangement fixed an artificial upper limit. However, we have estimated that the contribution from very high-energy particles is small. These estimates were made from radiochemical experiments where tritium was measured (or secondary reactions were studied) and from results on energy distributions on tritons between 50 and 150 MeV published by Genin *et al.*⁵ The energy spectra of ${}^4\text{He}$, ${}^3\text{He}$, and ${}^3\text{H}$ obtained at $\theta = 20^\circ$ for a gold target are given in Fig. 5. After the evaporation contribution has been subtracted, nonisotropic energy spectra are obtained, as shown in Fig. 6 for gold targets and Fig. 7 for a silver target.

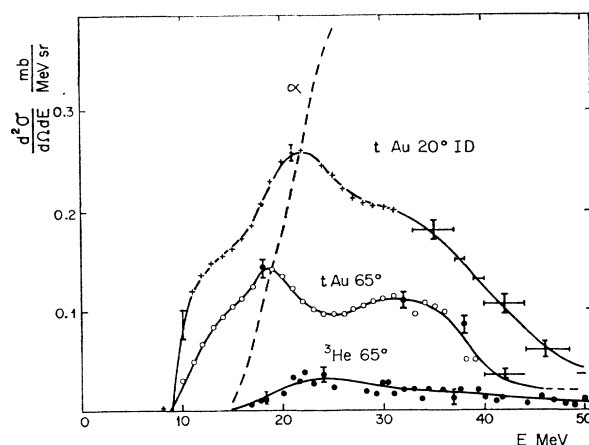


FIG. 6. Energy distribution of the nonisotropic process at $\theta_{\text{lab}} = 20^\circ$ and 65° for ${}^3\text{H}$ and ${}^3\text{He}$ from gold. Dashed line represents the ${}^4\text{He}$ spectrum.

A common feature for all these results is that the threshold is higher by 2 to 4 MeV than the threshold of the isotropic process, depending on whether the emitted particle is ${}^4\text{He}$ or ${}^3\text{H}$. This is a strong indication that we are not dealing now with a de-excitation mechanism in which the very high-level density allows the emission of particles far below the Coulomb barrier. Another feature can be pointed out: Cross sections are nearly the same from gold to thorium (40 ± 3 mb for ${}^4\text{He}$, 4 ± 0.5 mb for ${}^3\text{He}$, and 21 ± 3.5 for ${}^3\text{H}$).

On the other hand, the results for tritons cannot be explained by the same mechanism as for ${}^4\text{He}$ or ${}^3\text{He}$. Following Hess and Moyer,⁶ it seems reasonable to attribute the results for tritons to a secondary pickup mechanism. Prompt cascade nucleons, before leaving the nucleus, pickup one or two other nucleons. Energy spectra for tritons exhibit a rather strange shape with

⁵ J. Genin, P. Radvanyi, I. Brissaud, and C. Detraz, *J. Phys. Radium* **22**, 615 (1961).

⁶ W. N. Hess and B. J. Moyer, *Phys. Rev.* **101**, 337 (1956).

TABLE III. ^{197}Au nucleus model.

Concentric region No.	1	2	3	4	5	6	7
Radius (F)	$R_0 - 2.5$	$R_0 - 1.25$	$R_0 - 0.625$	R_0	$R_0 + 0.625$	$R_0 + 1.25$	$R_0 + 2.5$
Fermi well for protons (MeV)	34.82	33.83	30.87	25.57	17.84	10.45	4.10
Fermi well for neutrons (MeV)	45.50	44.70	40.33	33.41	23.31	13.66	5.36
Nuclear density of nucleons (F^{-3})	0.180	0.173	0.150	0.113	0.066	0.030	0.007

two peaks of widely different energy, although no such structure is found for deuterons. One explanation of the triton spectra may be attributed to two different formation processes. In the first process, a prompt proton picks up 2 neutrons directly, and in the second, a prompt proton picks up one neutron to form a deuteron, which in turn picks up another neutron before leaving the nucleus. The fact that ^3He particles are emitted up to high energies also favors either a pickup ($p+p+n$) process, or a stripping ($\alpha \rightarrow ^3\text{He}+n$) process. The latter is a secondary effect associated with the knockout of α particles from the nuclear surface. In any case, α -particle emission cannot be explained by a pickup process alone, since its cross section is much larger than that for both tritons and ^3He particles. Therefore these new results strengthen our conviction that the origin of nonisotropic ^4He particles is associated with a knockout mechanism.

IV. NUCLEON-CLUSTERING He SUBSTRUCTURES

A knockout mechanism for ejection of α substructures by prompt cascade nucleons was suggested some years ago by Perfilov and his collaborators.⁷ Also, more recently, experiments on $(\alpha, 2\alpha)$ reactions carried out by Igo *et al.*⁸ on copper and lead have confirmed the idea that one is observing such clusters, since the maximum of quasielastic events was found at the kinematic separation angle $\theta_1 + \theta_2 = 87.5^\circ$. These data and our results on spallation reactions over many years

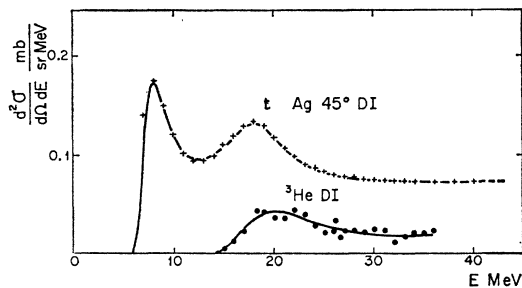


FIG. 7. Energy distribution at $\theta_{\text{lab}} = 45^\circ$ of ^3H and ^3He from silver.

⁷ V. I. Ostroumov, N. A. Perfilov, and R. A. Filov, Zh. Eksperim. i Teor. Fiz. **39**, 105 (1960) [English transl.: Soviet Phys.—JETP **12**, 77 (1961)].

⁸ G. Igo, L. F. Hansen, and T. J. Gooding, Phys. Rev. **131**, 337 (1963).

have lead us to develop a Monte Carlo program for prompt cascades where quasifree collisions between nucleons and α substructures on the nuclear surface are included.

Calculations start in the way described by Metropolis *et al.*,⁹ i.e., by the use of a mean free path and by treating quasifree nucleon scattering inside the nucleus in a Fermi potential. However, we have used the new diffuse-edge model proposed by Chen *et al.*¹⁰ Such a model describes nuclear matter density by a step function and gives a more realistic fit to Hofstadter's results on electron scattering.¹¹ The nuclear volume was decomposed into seven concentric shells, each with constant nuclear density. The corresponding radii and well depths for ^{197}Au are given in Table III.

Each concentric volume was considered as a distinct Fermi gas. Reflection and refraction were considered at each potential discontinuity. A more detailed description of the cascade calculations concerning prompt nucleons will be given elsewhere.¹²

In order to study the knockout of α clusters, we have made the assumption that on the nuclear surface, free scattering can occur between prompt nucleons and α clusters of nucleons. Several correlation probabilities were tried and the best fit was obtained with the values given in Table IV.

TABLE IV. Clustering probability for each concentric volume.

Region No.	1	2	3	4	5	6	7
Probability	0	0	0.0625	0.125	0.25	0.5	1

We attributed an average momentum to α substructures corresponding to an average kinetic energy of 10 MeV. Elastic and inelastic collisions between nucleons and α particles were treated, taking data from many p - α scattering studies. We assumed the following relation for both inelastic and elastic cross sections on helium:

$$\sigma_{n\alpha} = \sigma_{p\alpha} = 32.236/\beta^2 + 2.225/\beta - 7.017 \text{ (in mb)}$$

⁹ N. Metropolis, R. Bivins, M. Storm, A. Turkevich, J. M. Miller, and G. Friedlander, Phys. Rev. **110**, 185 (1958).

¹⁰ K. Chen, Z. Fraenkel, G. Friedlander, J. R. Grover, J. M. Miller, and Y. Shimamoto (private communication). Also, J. P. Cohen, G. Alboni, M. Gusakov, and L. Valentin, Phys. Letters **15**, 255 (1965).

¹¹ R. Hofstadter, Rev. Mod. Phys. **28**, 214 (1956).

¹² J. P. Cohen (thesis in preparation, Paris-Orsay) (unpublished).

which yields about 260 mb for $\beta \approx 0.352$. Differential cross sections $d^2\sigma/d\Omega d\epsilon$ have been measured by several authors, and we have found that the following equations give a rather good representation of the data:

$$d^2\sigma/d\Omega dE = Ke^{2.94} \quad \text{for } \theta_{c.m.} < 10^\circ,$$

$$d^2\sigma/d\Omega dE = K'Be^{-p\theta} + Ce^{q(\theta-\pi)} \quad \text{for } 10^\circ < \theta_{c.m.} < 180^\circ,$$

where K and K' are normalization parameters and B , C , p , and q were tabulated for each E value before the computation.

The α - α' scattering events were calculated with the cross-section equation:

$$\sigma_{(\alpha,\alpha)} = (3 \times 1/\beta^2 + 20) F^2$$

and angular distributions were taken from experimental results on $d^2\sigma/d\theta dE$ given by the (α,α') scattering studies, mainly between 50 and 120 MeV by Darriulat *et al.*¹³

The only inelastic events which were taken into account correspond to the stripping processes into ($^3\text{He}+n$) or ($^3\text{H}+p$). One of the main difficulties is the choice of the potential barrier for α particles. We calculated a Coulomb height for a nucleus of radius $1.30A^{1/3}\text{F}$. This is certainly too high for alpha clusters located in the very diffuse edge. In order to compensate for such an inhibition effect, no reflection restriction was applied to the Coulomb height for the α -particle exit. Using these approximations, the energy distribution for α particles ejected at all angles from gold nuclei by 155-MeV protons was computed and compared with the experimental integrated energy spec-

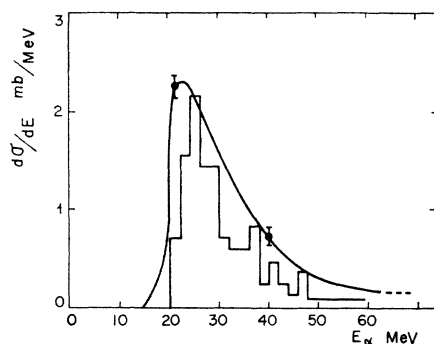


FIG. 8. Energy distribution (integrated in angles) of prompt knockout alpha particles. The steps are found by Monte Carlo calculations and the curved line corresponds to the experimental results.

¹³ P. Darriulat, G. Igo, H. G. Pugh, and H. D. Holmgren, *Phys. Rev.* **137**, B315 (1965).

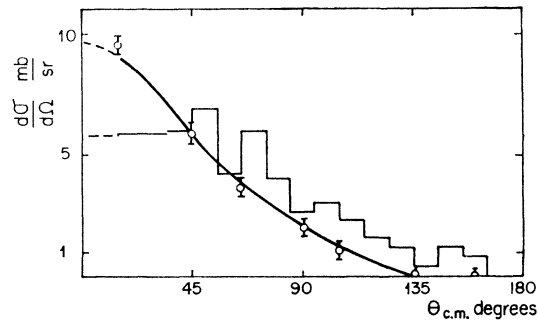


FIG. 9. Angular distribution of α particles in a knockout process. Experimental results are given on the curved line and calculated data are represented by the histogram.

trum.¹ Figure 8 shows such a comparison with the correlation probability given in Table IV. Although the total calculated cross-section value of 30 mb is still a bit smaller than the experimental result of 37 mb, the energy distribution follows the experimental spectrum very well. The clustering effect involves a correlation of about 20 to 25 nucleons into 5 to 6 α substructures, at least during the time of collision with prompt nucleons.

As illustrated by Fig. 9, the angular distribution does not agree with the computed data as well as the energy distribution does. However, it should be pointed out that there are gross assumptions in the calculation of the direction of emitted particles (Coulomb scattering was neglected).

It should be emphasized that nucleon-clustering effects are observed in highly energetic collisions and no conclusion can be drawn as to the existence of *stable* α substructures inside heavy nuclides in their fundamental levels. The correlations into α clusters might appear at the very moment of the impact of prompt cascade nucleons on the excited outer part of the nucleus, although such a nucleus in its ground state could still be described in the general picture of the shell model.

ACKNOWLEDGMENTS

It is a pleasure for the authors to acknowledge the benefit of stimulating conversations on prompt-cascade computations and on the evaporation theory with R. Da Silveira, I. Dostrovsky, and Z. Fraenkel. Our thanks are also due to J. Peter, who helped in various stages of the experiments. We are most grateful to J. R. Huizenga for discussing our manuscript carefully and giving us most valuable advice.